International Journal of
INTELLIGENT SYSTEMS AND APPLICATIONS IN ENGINEERING
ISSN:2147-6799 www.ijisae.org Original Research Paper

Effect of Mass Transfer and Heat Sources on the Rotatory Flow Past an Accelerated Infinite Vertical Plate through Porous Medium

Pratibha P. Ubale Patil[1], Dr. Vinod Kulkarni [2], Dr R.M. Lahurikar [3,*]

Submitted: 13/08/2024 **Revised:** 25/09/2024 **Accepted:** 03/10/2024

Abstract: The Laplace transform approach has been used to develop an accurate solution to the unsteady free convection flow of a viscous incompressible fluid in the presence of foreign mass via a porous media past an infinite vertical isothermal plate that was initiated impulsively in a rotating fluid. Numerical values of skin friction are presented in a table, and graphs display axial and transverse velocity profiles. As the permeability parameter λ increases, the air's transverse velocity decreases in magnitude, and same for rotational parameter Rc.Consequently, when the porous medium is denser than when air or water flows as an infinite medium, the flow is slow down for λ increases. It is observed that the axial velocity for both water and air becomes irregular as the rotating parameter Rc decreases, that the Coriolis forces physically interrupt fluid motion, that the axial velocity-driven flow of Rc is unstable because of a point of inflection on the axial velocity profiles of both water and air, which makes the flow turbulent, and that the flow caused by the transverse velocity is unstable when Rc < 1. As the Prandtl number Pr increases, the axial velocity falls. When Schmidt number Sc increases, axial velocity falls for both air and water, but when Sc increases, transverse velocity becomes unstable for air. It is observed that decrease in N, the ratio of chemical species diffusion to thermal diffusion, leads to an increase in the axial velocity because the buoyant force facilitates the movement of air but Transverse velocity decreases for increase in N. As N decreases, axial velocity, and transverse velocity decreases for water. S increases then flow become unstable for both water and air. If Rc increases, axial skin friction becomes irregular and transverse skin friction increases for air but for water axial skin friction and Transverse skin friction both oscillates. Axial skin friction oscillates and transverse skin friction decreases for buoyancy force parameter N for water, and for air, axial skin friction and transverse skin friction oscillates. As permeability parameter λ increases, axial and transverse skin friction decrease for water, and for air axial velocity decreases and transverse skin friction increases. Axial skin friction rises with rise in heat source parameter S whereas Transverse skin friction oscillates as S rises.

Keywords: *Heat transfer, Heat sources, Mass transfer, Porous medium, Incompressible fluid, Coriolis force*

1. Introduction

The flow of an incompressible fluid past an infinite horizontal plate was first studied by Stokes [1] who presented an exact solution of Navier-Stokes equation. Analytical solution to this problem in case of semi-infinite horizontal plate was given by Stewartson([2] and [3]), whereas finite difference solution of the flow past a semi-infinite horizontal plate was presented by hall [4]. Tani and Yu [5] solved this problem by integral method.

Numerous writers have examined the natural convection flow of a viscous incompressible fluid past an infinite vertical plate; this topic has been covered in numerous research papers and books on heat transfer (e.g. Ghebart, [6], Bejan [7]). How does the impulsive motion occur if it is applied to an isothermal vertical plate that is surrounded by a stationary mass of fluid? Soundalgekar [8] was

1 Research Scholar, Dr. Babasaheb Ambedkar Marathwada University, Chh.Sambhajinagar
2 Principal, Uttamchand Bagdiya College, Risod
3Associate Professor, Govt College of Arts and Science, Chh.Sambhajinagar
**Corresponding author: vbhalerao2010@gmail.com (Dr. Vinod Kulkarni)*

the first to study this using the Laplace transform approach, examining the impact of free convection current close to the plate. Due to its significance in industry, the convective heat transfer potential of flow through porous medium is a relatively recent topic that has drawn the attention of numerous researchers over the past 30 years. With today's porous insulating technologies, as energy costs increased and cooling strategies for drying porous materials like wheat and improved oil were minimized, as well as issues with storing heat-generating materials like coal and grains, natural gas-cooled electronic equipment and nuclear reactors expanded. Understanding fluid flow, heat transfer, and mass transfer is essential for many industrial operations, such as reservoir engineering, which enhances subterranean water and oil production. Numerous studies have examined natural convection through porous media, and earlier research has employed models like the Darcy flow model to understand flow through porous media. Rotating fluids, including the impact of Coriolis forces, have also been studied in this way. Mass transfer has been the subject of some research in a variety of situations, such as Park and Lau [9] investigated experimentally how the distribution of mass transfer is affected by the rotational Coriolis force. More recently, Bhalerao and Lahurikar [10] investigated the impact of mass transfer on transient flow across an infinite vertical plate in a spinning fluid. Isothermal fluxes in rotating porous media have been the subject of little research, as demonstrated by Vadasz [11] and Bejan [12]. Additionally, the study is pertinent to geophysical applications including atmospheric and ocean circulation.

Srinivasa Raju et al. [13] investigate how unstable MHD free convection flow past an infinite vertical plate is affected by thermal radiation and heat sources. Analytical and numerical solutions for unsteady MHD free convection flow via an exponentially moving vertical plate were discovered by Srinivasa Raju and Gorla [14]. Sheri and Srinivasa Raju [15] discovered that viscous dissipation affected the transient free convection flow through a porous media via an infinite vertical plate. Raju et al. [16] investigated the use of the finite element approach for unsteady MHD free convection flow past a porous plate that is inclined vertically. According to Srinivasa Raju et al. [17], the unstable hydromagnetic natural convection Couette flow was also numerically solved. Studies on chemical reactions and nanofluids are also visible. The numerical solution for unsteady MHD natural convection heat and mass transfer is provided by Reddy et al. [18]. The impact of chemical reactions on unsteady fluid flow across an exponentially accelerated vertical plate was discovered by Srinivasa Raju et al. [19]. Dodda et al. [20] investigated heat transfer and MHD boundary layer flow of nanofluid over a nonlinear stretching sheet.

The impact of free convection currents on the impulsive motion of an infinite vertical plate given a motion in a stationary fluid was previously examined by Soundalgekar [8]. The impact of free convection currents on the motion of an infinite vertical plate with accelerated motion was examined by Soundalgekar and Gupta [21]. The equations controlling fluid flow in the presence of foreign mass were derived by Gebhart et al. in [22]. The impact of mass transfer on a steady free convection flow via a semi-infinite vertical plate was investigated by Gebhart and Pera [23]. Soundalgekar, Pohanerkar, and Lahurikar [25)] investigated how heat sources and mass transfer affected the flow past an accelerating infinite plate. Lahurikar, Gitte, and Ubale Patil [24], investigated the effect of mass transfer on flow through a porous media past an infinite vertical plate that was initiated impulsively in a rotating fluid. The impact of mass transfer on the Stokes problem for an infinite vertical plate in a rotating fluid was also examined by Lahurikar, Gitte, and Ubale Patil [26].

The need to comprehend this physical scenario stems from the lack of study on isothermal flow in rotating porous media and the limited literature on the effects of mass transfer and heat sources on the flow of a fluid past an infinite vertical plate that is evenly accelerated. Investigating how heat sources and mass transfer affect the rotatory flow past an accelerated infinite vertical plate through a porous media is the aim of the current investigation.

2. Mathematical Analysis

Consider an infinite vertical plate embedded in a porous medium surrounded by a viscous incompressible system. Suppose the X'-axis is in vertical upward direction along the accelerated plate, Y' is horizontal perpendicular to X'- axis and Z'- is Axis which is normal to the X'-Y' plane.

Initially plate and fluid are stationary and is with uniform initial temperature T'_∞. Initially fluid concentration level is C'_∞ and porous medium is at steady state. At the time $t' > 0$,plate undergoes uniform acceleration in vertical direction, simultaneously temperature raised to constant temperature T'_w and concentration level raised to C'_w and fluid starts moving along Z' axis very slowly with angular velocity Ω'. At the plate is infinite except all the physical variables are functions of Z' and t'. Fluid in porous medium is viscous and incompressible and it has uniform porous medium distribution. Fluid has uniform angular velocity Ω'.When fluid moves due to rotation of earth steadily, the coriolis forces oppose the displacement of fluid element and right angle to both the axis of rotation. On a fluid centrifugal forces are acting for slowly rotating system and if the system is rotating very slowly, the square and higher order rotational terms in the centrifugal forces maybe neglected.

Since the plate is infinite in size, heat sources are combined and inertia terms are insignificant. The flow can then be demonstrated to be controlled by the following set of equations under standard Boussinesq's approximation, ignoring viscous dissipation heat and the Sorate-Dufur effect (Gebhart and Pera, [23]).

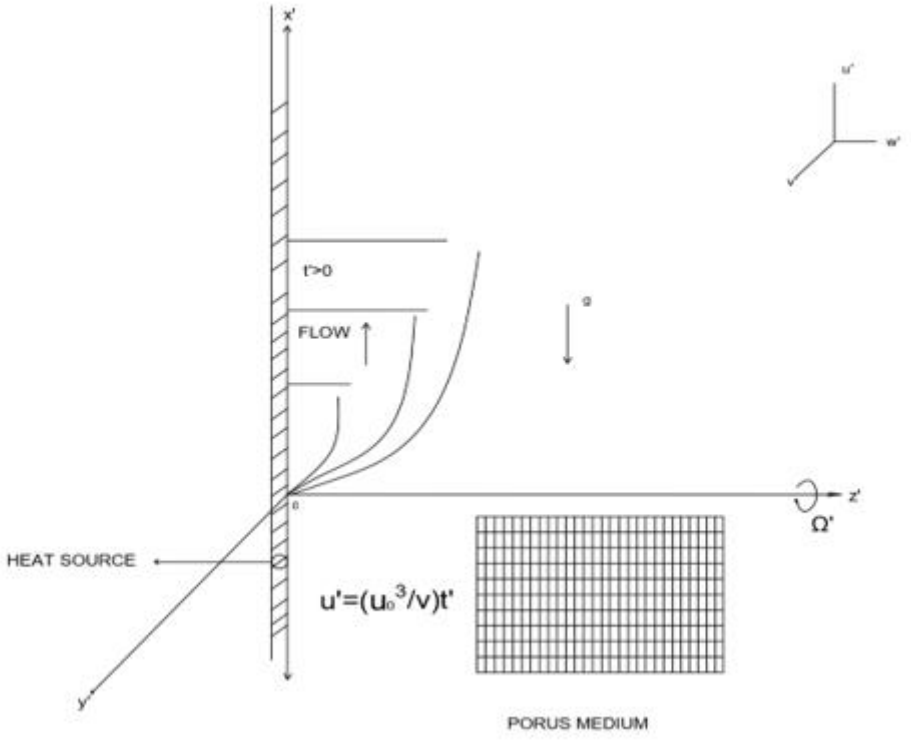

Figure 1: Geometry of problem

Following Gebhart and Pera [23], we can show that under usual Boussinesq approximations the unsteady free convection flow is governed by a system of coupled partial differential equations:

$$\frac{\partial u'}{\partial t'} - 2\Omega' v' = g\beta\left(T' - T'_\infty\right) + g\beta^*\left(C' - C'_\infty\right) + \nu\frac{\partial^2 u'}{\partial z'^2} - \frac{\nu}{\kappa}u' \qquad (1)$$

$$\frac{\partial v'}{\partial t'} + 2\Omega' u' = \nu\frac{\partial^2 v'}{\partial z'^2} - \frac{\nu}{\kappa}v' \qquad (2)$$

$$\rho C_P\frac{\partial T'}{\partial t'} = K\frac{\partial^2 T'}{\partial z'^2} + S_1(T' - T'_\infty) \qquad (3)$$

$$\frac{\partial C'}{\partial t'} = D\frac{\partial^2 C'}{\partial z'^2} \qquad (4)$$

The initial and boundary conditions are

$$t' \le 0, u' = 0, T' = T'_\infty, C' = C'_\infty \qquad \text{for all } Z'$$

$$t' > 0, u' = \left(\frac{U_0^3}{\nu}\right)t', T' = T'_w, C' = C'_w \qquad \text{at } Z'=0$$

$$u' = 0, T' \to T'_\infty, C' \to C'_\infty \qquad \text{as} \quad Z' \to \infty \qquad (5)$$

Here, u' is the velocity components along the X' and v' is the velocity of Y' axis respectively, g is the acceleration due to gravity, β is the coefficient of volume expansion,β^* is the coefficient of volume expansion with concentration,T' is the fluid temperature near the plate,C_∞ the mass concentration in the fluid far away from the plate, ν the kinematic viscosity, C_P is the specific heat at constant pressure,K is thermal conductivity, D is the mass diffusivity,U_0 is the impulsive velocity of the plate, ,κ is the coefficient of permeability (which is constant and increases with the ease of percolation; the conditions under which ,κ can be taken at constant are discussed by Muskat [27]), and ρ is the density.

On introducing the following nondimensional quantities

$$\text{U}=\frac{u'}{U_O}\ ,\ \text{v}=\frac{v'}{U_O}\ ,\ \text{t}=\frac{t'}{\nu}GU_O^2\ ,\ \text{z}=\frac{z'U_O\sqrt{G}}{\nu}\ ,\ \text{Pr}=\frac{\mu C_p}{K}$$

$$\text{G}=\frac{\nu\beta g(T'_w-T'_\infty)}{U_O^3},\ \theta=\frac{(T'-T'_\infty)}{(T'_w-T'_\infty)}\ ,\text{Rc}=\frac{\Omega'\nu}{GU_O^2}=\frac{1}{GR_OR_e}\ ,\text{S}=S_1\nu^2/kU_O^2 \qquad (6)$$

$$\text{Sc}=\frac{\nu}{D},\ \text{C}=\frac{(C'-C'_\infty)}{(C'_w-C_\infty)},\text{N}=\frac{\beta^*(C'_w-C'_\infty)}{\beta(T'_w-T'_\infty)}\ ,K^*=\frac{\nu}{\kappa U_O^2},\lambda=\frac{K^*}{G}$$

C is the nondimensional mass concentration, G is the Grashof number, N is the ratio of buoyancy forces, θ is the nondimensional temperature, Sc is the Schmidt number, Ro is the Rossby number, Re is the Reynolds number, and Rc is the rotational parameter caused by Coriolis forces. When the porous medium is denser, the porous medium parameter, λ, is larger.

Equation (1) – (5) reduce to the following nondimensional form

$$\frac{\partial u}{\partial t} - 2Rcv = \frac{\partial^2 u}{\partial z^2} + \theta + NC - \lambda u \qquad (7)$$

$$\frac{\partial v}{\partial t} + 2Rcu = \frac{\partial^2 v}{\partial z^2} - \lambda v \qquad (8)$$

$$Pr\frac{\partial\theta}{\partial t} = \frac{\partial^2\theta}{\partial z^2} + \text{S}\theta \qquad (9)$$

$$Sc\frac{\partial C}{\partial t} = \frac{\partial^2 C}{\partial z^2} \qquad (10)$$

The initial and boundary conditions are

$t \le 0, u = 0, \theta = 0, C = 0$ For all Z

$t > 0, u = \frac{t}{G}, \theta = 1, C = 1$ as Z=0

$u = 0, \theta = 0, C = 0$ as Z→ ∞ (11)

Now we combine (7) and (8) by introducing q=u+iv, which then reduce to

$\frac{\partial q}{\partial t}$ + 2iRcq =θ +$\frac{\partial^2 q}{\partial z^2}$ - λq + Nc (12)

Pr $\frac{\partial \theta}{\partial t}$ =$\frac{\partial^2 \theta}{\partial z^2}$ + Sθ (13)

Sc $\frac{\partial c}{\partial t}$ =$\frac{\partial^2 c}{\partial z^2}$ (14)

The initial and the boundary conditions are

t ≤ 0 ,q = 0,θ =0, c = 0 for all z

t ≥ 0, q =$\frac{t}{G}$, θ = 1, c = 1, at z=0

q = 0, θ = 0, c = 0 as z→ ∞

The solutions of equations (12) – (14) satisfying initial and boundary conditions are derived by the usual Laplace transform technique

C = erfc ($\eta\sqrt{Sc}$)

θ=$\frac{1}{2}$ $\{e^{-\sqrt{pr\alpha t}(2\eta)}$erfc ($\eta\sqrt{pr}$ -$\sqrt{\alpha t}$) + $e^{\sqrt{pr\alpha t}(2\eta)}$erfc ($\eta\sqrt{pr}$ + $\sqrt{\alpha t}$)$\}$

q=$\frac{t}{2G}$ ($e^{-\sqrt{b_1 t}(2\eta)}$erfc (η -$\sqrt{b_1 t}$) + $e^{\sqrt{b_1 t}(2\eta)}$erfc (η +$\sqrt{b_1 t}$)) - $\frac{\eta\sqrt{t}}{2G\sqrt{b_1}}$ $\{e^{-\sqrt{b_1 t}(2\eta)}$erfc ($\eta$ -$\sqrt{b_1 t}$) - $e^{\sqrt{b_1 t}(2\eta)}$erfc (η +$\sqrt{b_1 t}$)$\}$ - $\frac{N}{2c\,(Sc-1)}\Big\{$ $e^{-\sqrt{b_1 t}(2\eta)} erfc\left(\eta - \sqrt{b_1 t}\right)$ + $e^{\sqrt{b_1 t}(2\eta)} erfc\left(\eta + \sqrt{b_1 t}\right)\Big\}$+ $\frac{Ne^{ct}}{2c(Sc-1)}\{$ $e^{-\sqrt{(c+b_1)t}(2\eta)}$erfc ($\eta$ -$\sqrt{(c+b_1)t}$) + $\{$ $e^{\sqrt{(c+b_1)t}(2\eta)}$erfc ($\eta$ +$\sqrt{(c+b_1)t}$)$\}$ - $\frac{1}{a(pr-1)}\{$ $e^{-\sqrt{b_1 t}(2\eta)}$erfc (η-$\sqrt{b_1 t}$) + $e^{\sqrt{b_1 t}(2\eta)}$erfc (η+$\sqrt{b_1 t}$)$\}$ + $\frac{e^{at}}{2a(pr-1)}$ $\{e^{-\sqrt{(a+b_1)t}(2\eta)}$erfc ($\eta$ - $\sqrt{(a+b_1)t}$) + $e^{\sqrt{(a+b_1)t}(2\eta)}$erfc ($\eta$ +$\sqrt{(a+b_1)t}$)$\}$ + $\frac{N}{b_1}$ erfc($\sqrt{Sc}\,\eta$) - $\frac{Ne^{ct}}{2c(Sc-1)}\{e^{-2\eta\sqrt{ctSc}}$erfc($\eta\sqrt{Sc}$ - $\sqrt{ct}$)+ $e^{2\eta\sqrt{ctSc}}$erfc($\eta\sqrt{Sc}$ + $\sqrt{ct}$)$\}$ + $\frac{1}{2a(pr-1)}\{e^{-2\eta\sqrt{\alpha tpr}}$ erfc ($\eta\sqrt{pr}$ -$\sqrt{\alpha t}$) + $e^{2\eta\sqrt{\alpha tpr}}$ erfc ($\eta\sqrt{pr}$ +$\sqrt{\alpha t}$)$\}$ - $\frac{e^{at}}{2a(pr-1)}\{e^{-\sqrt{pr(a+\alpha)t}(2\eta)}$ erfc($\eta\sqrt{pr}$ -$\sqrt{(a+\alpha)t}$) + $e^{\sqrt{pr(a+\alpha)t}(2\eta)}$erfc ($\eta\sqrt{pr}$ +$\sqrt{(a+\alpha)t}$)$\}$

Where, $\eta = \frac{z}{2\sqrt{t}}$, $b_1 = \lambda + 2iRc$, c=$\frac{b_1}{Sc-1}$,a= $\frac{s+b_1}{Pr-1}$

To gain physical insight, we have separated q into real and imaginary parts with the help of formulas given by Lahurikar [28] and computed numerical values of u and v.

We assumed the fluid to be viscous incompressible i.e air (Pr = 0.71 when Mach number Ma ≪ 1) and water (Pr= 7). The values

of Schmidt number Sc are given by Bejan (12)
(Table 1).

Table 1: The values of Schmidt number Sc adapted from Bejan [12]

Pr	Species at Low Concentration 1 atm, app 25^0C	Sc
0.71	Hydrogen,H_2	0.22
	Water Vapour,H_2O	0.60
	Ammonia,NH_3	0.78
	Carbon dioxideCO_2	0.94
	Methanol, CH_3OH	0.99
7.0	Hydrogen,H_2	152
	Oxygen,O_2	356
	Carbon dioxide, CO_2	453
	Chlorine, cl	617
	Calcium chloride, $CaCl_2$	750

From the velocity field, the skin friction is obtained in nondimensional form as

$$2\sqrt{t}\,\tau = -\frac{dq}{d\eta}|\eta = 0 = -(\tau_x + \tau_y)$$

Where$\tau = \frac{\tau'\sqrt{G}}{\rho U_0} - \frac{dq}{d\eta|_{\eta=0}} = \frac{t}{G}\left(-\frac{2}{\sqrt{\pi}}e^{-b_1 t} - 2\sqrt{b_1 t}\ erf\sqrt{b_1 t}\right) + \frac{N}{b_1}\left[-\frac{2}{\sqrt{\pi}}e^{-b_1 t} - 2\sqrt{b_1 t}\ erf\sqrt{b_1 t}\right] + \frac{Ne^{ct}}{b_1}\left[-\frac{2}{\sqrt{\pi}}e^{-(c+b_1)t} - 2\sqrt{(c+b_1)t}\ erf\sqrt{(c+b_1)t}\right] + \frac{1}{(s+b_1)}\left[-\frac{2}{\sqrt{\pi}}e^{-b_1 t} - 2\sqrt{b_1 t}\ erf\sqrt{b_1 t}\right] + \frac{e^{at}}{(s+b_1)}\left[-\frac{2}{\sqrt{\pi}}e^{-(a+b_1)t} - 2\sqrt{(a+b_1)t}\ erf\sqrt{(a+b_1)t}\right] - \frac{2}{\sqrt{\pi}}\frac{N}{b_1} + \frac{Ne^{ct}}{b_1}\left[-\frac{2}{\sqrt{\pi}}e^{-ct} - 2\sqrt{Sc}\sqrt{ct}\ erf\sqrt{ct}\right] + \frac{1}{(s+b_1)}\left[-\frac{2}{\sqrt{\pi}}e^{\frac{st}{Pr}} - 2i\sqrt{st}\left(i\sqrt{\frac{st}{Pr}}\right) + \frac{e^{at}}{(s+b_1)}\left[-\frac{2}{\sqrt{\pi}}e^{-(a+\alpha)t} - 2\sqrt{Pr}\sqrt{(a+\alpha)t}\ erf\sqrt{(a+\alpha)t}\right]\right]$$

Where , , $b_1 = \lambda + 2iRc$, c=$\frac{b_1}{Sc-1}$,a= $\frac{s+b_1}{Pr-1}$

We have separated τ into real and imaginary parts as axial skin friction τ_x and $\tau_y$transverse skin friction formulas given by lahurikar [28] we have computed value of τ_x and τ_y and these are listed in Table (2) and Table (3)

3. Results and discussion

3.1 Results

In figure 2-24, the velocity profiles are displayed.The results of behaviour of axial velocity and Transverse velocity are given below:

1) When all other parameters are held constant, axial velocities are displayed for a range of

Schmidt number values. The axial velocities of air (figure 2) are found to decrease as Sc increases.

2) The axial velocity decreases as the Prandtl number Pr rises(figure 3).

3) The axial velocities of water (figure 4) is found to decrease as Sc rises. As Rc rises axial velocity also rises.

4) Transverse velocity exhibits instability as Sc fall (figure 5).

5) Transverse velocity decreases as Schmidt number Sc rises (figure 6).As Rc uprises transverse velocity falls.

6) The buoyant force N increases flow of air (figure 7) increases.

7) For water (figure 8), it is noticed that there is decrease in N, results in decrease in the axial velocity.

8) The air's transverse velocity decreases in magnitude as N rises (figure 9).

9) As the ratio of buoyancy force N grows, so does the water's transverse velocity (figure 10).

10) It is noted that for air (figure 11) flow is irregular as Rc increases whereas for water (figure 13), the axial velocity becomes irregular as the rotating parameter Rc decreases.

11) In (figure 12) rotating parameter λ increases axial velocity decreases.

12) For water (figure 13), the axial velocity becomes irregular as the rotating parameter Rc decreases.

13) It is physically accurate that the Coriolis forces interrupt fluid motion. Additionally, it is noted that Rc's axial velocity-driven flow is unstable due to a point of inflection on the axial velocity profiles of both water (figure 15) and air (figure 14), which causes the flow to become turbulent. According to the same conclusion, the flow caused by the transverse velocity is unstable when Rc < 1. In this case, inertia forces dominate the Coriolis forces, resulting in a large product of the nondimensional Rossby number and the Reynolds number. The flow slows down as the Prandtl number rises.

14) As time t decreases, the axial velocity of air decreases (figure 16).

15) The magnitude of the air's transverse velocity falls with increasing time t (figure 17).

16) As time t decreases axial velocity of water decreases(figure 18).

17) The magnitude of the air's transverse velocity drops as the permeability parameter λ rises (figure 19) and the same is true for the rotational parameter Rc (figure 20) so, the drop is larger for high λ when the porous media is denser in air (figure 19) or water (figure 21) is flowing as an infinite medium.

18) The transverse velocity of water decreases as λ increases (figure 22).

19) Heat source parameter S increases the flow become unstable for both water and air. (figure 23 and figure 24)

By using Lahurikar's formulae [28] we have separated τ_x and τ_y for which using different values of Rc, Sc, λ and other parameters we found values of axial and transverse skin friction, we enlisted Table (2) and Table (3). The observations are given here:

As time t increases axial skin friction increases for both water and air whereas Transverse skin friction decreases for both air and water. For buoyancy force parameter N axial skin friction oscillates and Transverse skin friction also decreases for water, also axial skin friction and Transverse skin friction both oscillates for air. As Coriolis force parameter Rc increases Axial and transverse skin friction both become unstable for air. But if Rc increases axial skin friction and Transverse skin friction is irregular for water. As permeability parameter λ increases axial skin friction and Transverse skin friction decreases for water and for air axial skin friction decreases and Transverse skin friction increases. From table we also observe that increase in Sc leads to decrease in both axial friction and transverse skin friction of

water also decreases in axial friction of air except for Methanol whereas with increase in Sc Transverse velocity become instable for air. The axial skin friction increases with increase in heat source S but Transverse skin friction become unstable with rising S.

3.2 Figures and tables

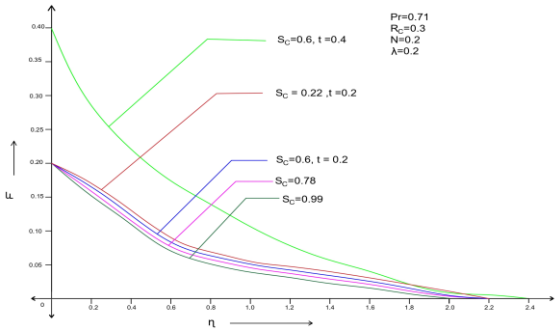

Figure 2:- Axial velocities are shown for different values of Schmidt number Sc of air. An increase in Sc leads to a decrease in the axial velocity.

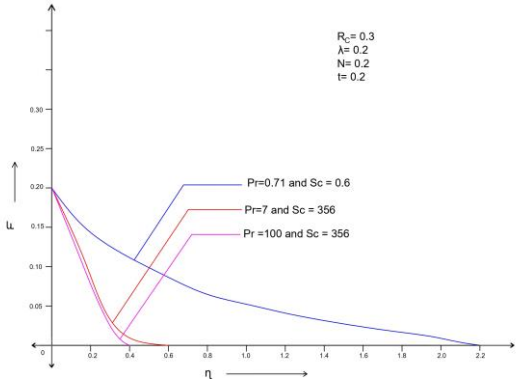

Figure 3:- As the Prandtl number Pr increases the flow slows down.

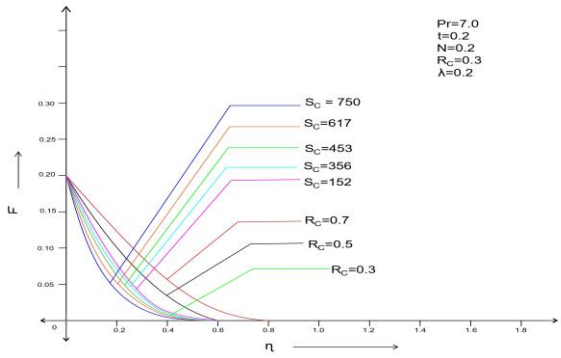

Figure 4: - Axial velocities are shown for different values of Schmidt number Sc of water. An increase in Sc leads to decrease in axial velocity. As Rc increases axial velocity also increases.

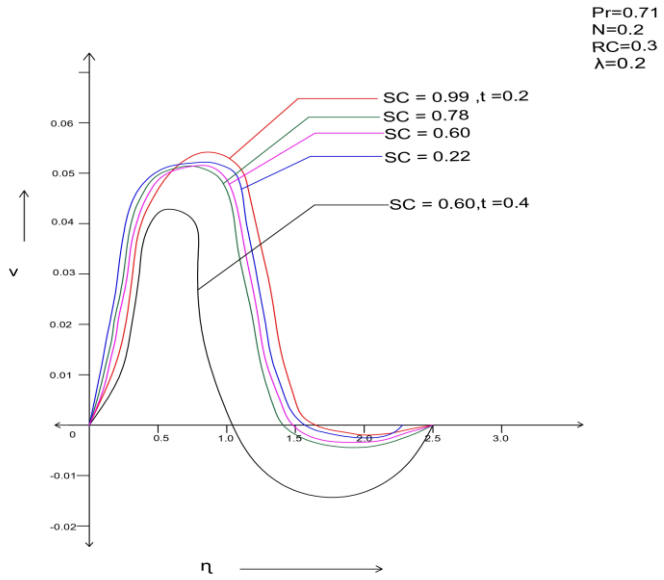

Figure 5:- Decrease in the Schmidt number Sc shows instability in the transverse velocity of air.

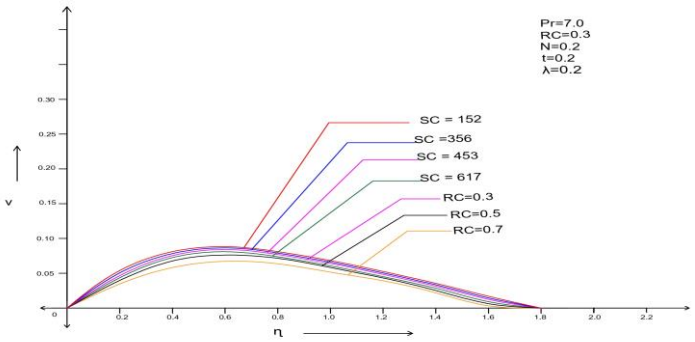

Figure 6:- An increase in the Schmidt number Sc shows decrease in Transverse velocity. As Rc increases Transverse velocity decreases.

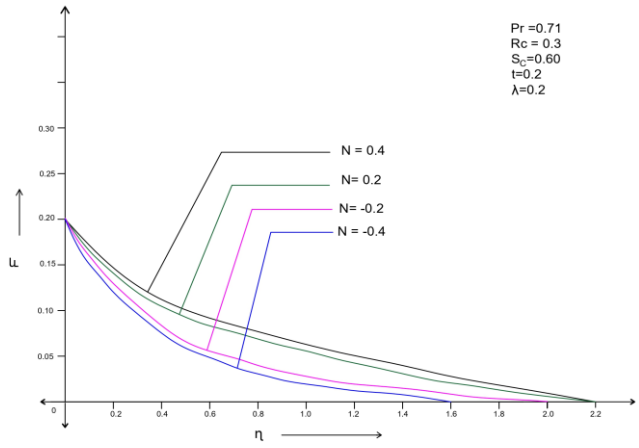

Figure 7:- For air, as buoyancy force N decreases, axial velocity falls down

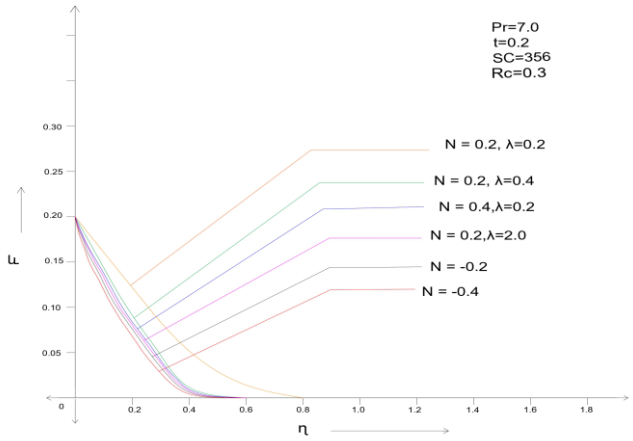

Figure 8:- Axial velocity of water decreases with an decreases in ratio of buoyancy forces N.

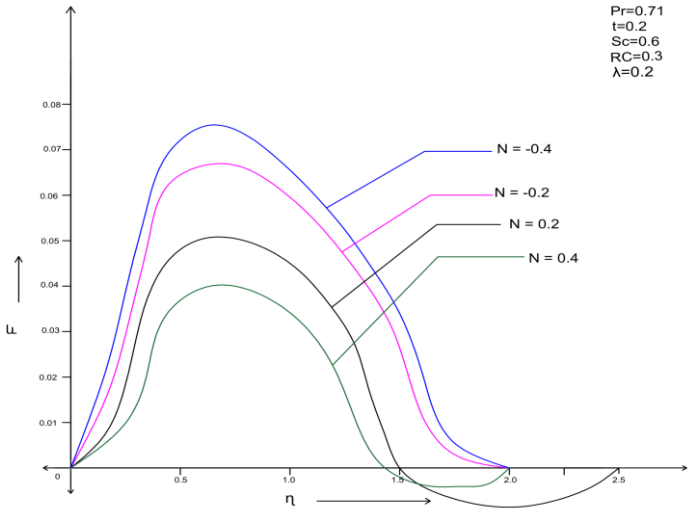

Figure 9:- Transverse velocity of air decreases with an increase in the ratio of buoyancy forces N.

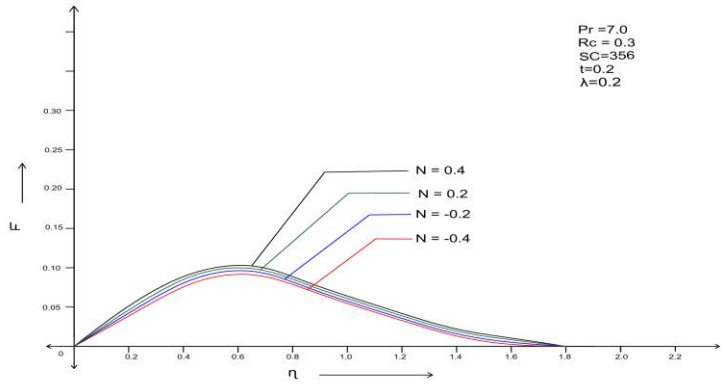

Figure 10:- Transverse velocity of water decreases with decrease in ratio of buoyancy forces N.

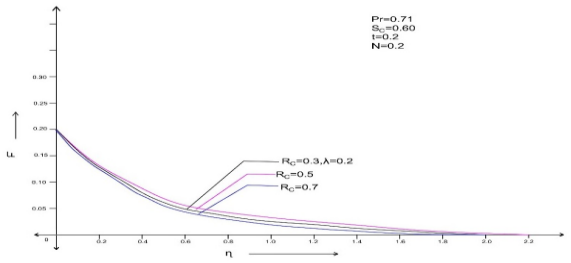

Figure 11: For air, rotating parameter Rc increases then flow is irregular.

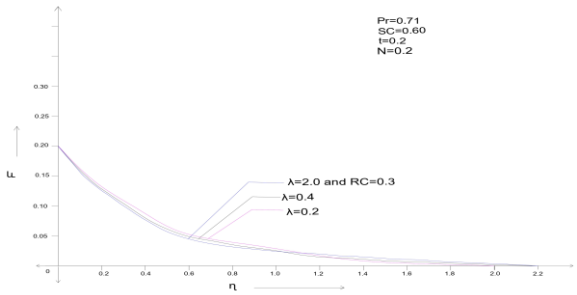

Figure 12 :- As permeability parameter or the resistance of the porous medium increases ,the axial velocity of air decreases.

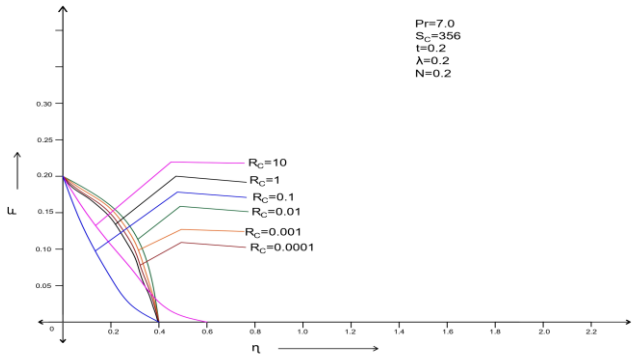

Figure 13:- The rotating parameter Rc decreases then flow is irregular.

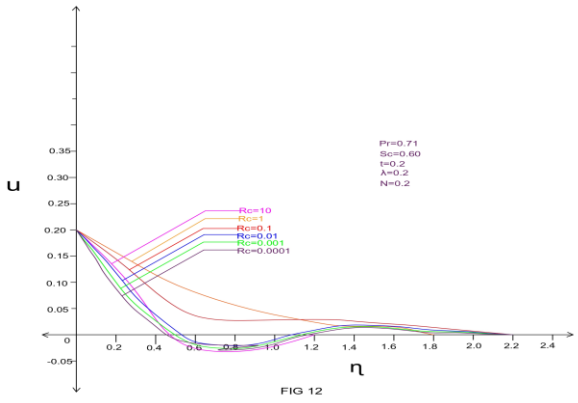

Figure 14 :- As Rc decreases axial velocity-driven flow is unstable.

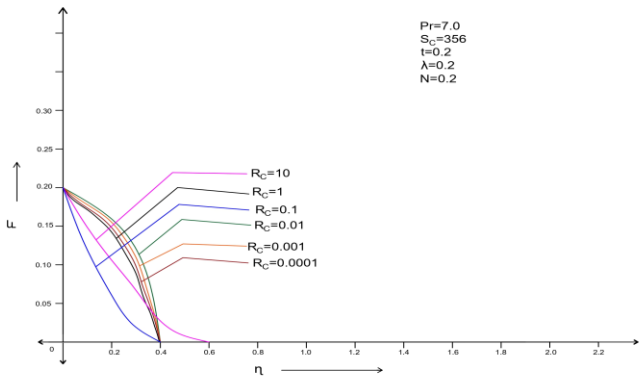

Figure 15:- As Rc decreases axial velocity-driven flow for water is irregular

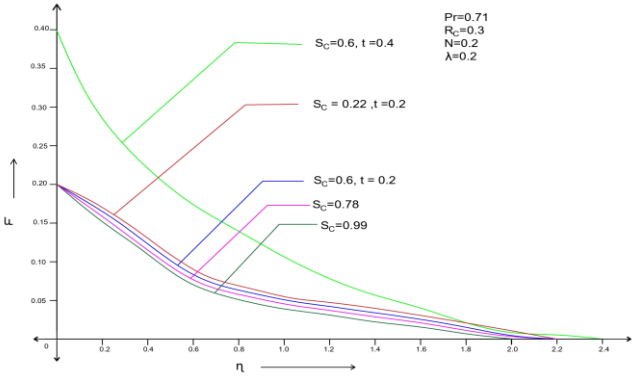

Figure 16:- As time t decreases , the axial velocity of air also decreases.

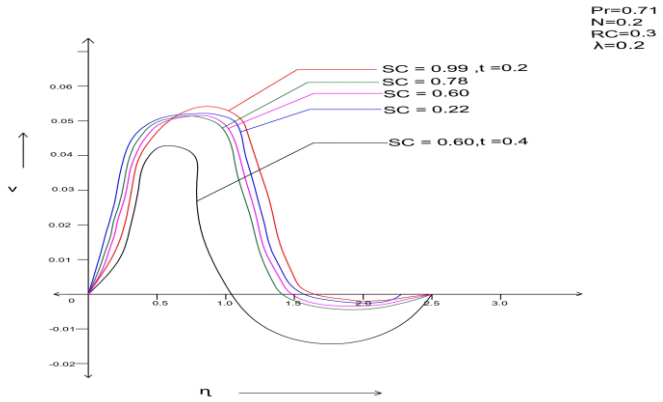

Figure 17 :- As time t increases ,the magnitude of the Transverse velocity of air decreases..

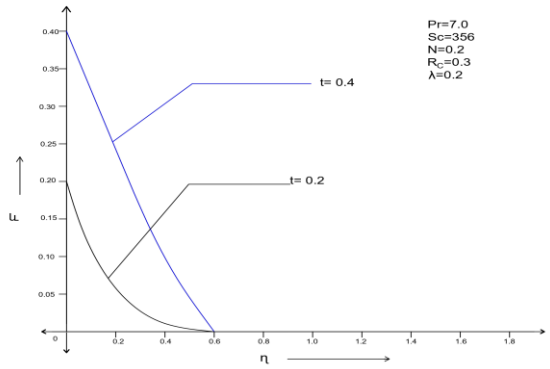

Figure 18:- As time t decreases axial velocity also decreases.

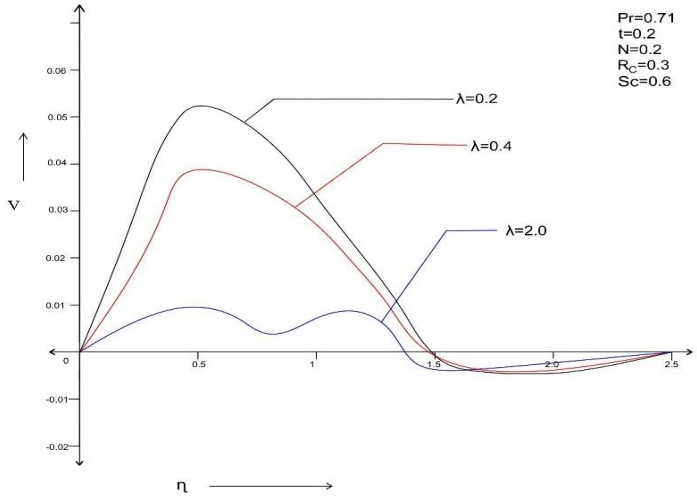

Figure 19 :- As permeability parameter increases , the magnitude of the Transverse velocity of air decreases.

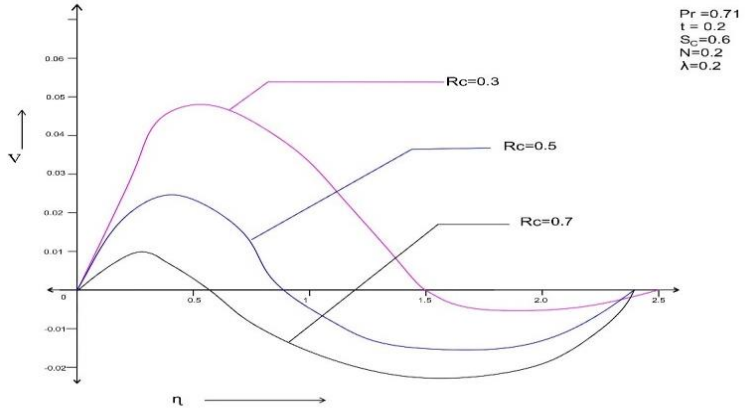

Figure 20 :- As rotating parameter Rc increases , Transverse velocity decreases

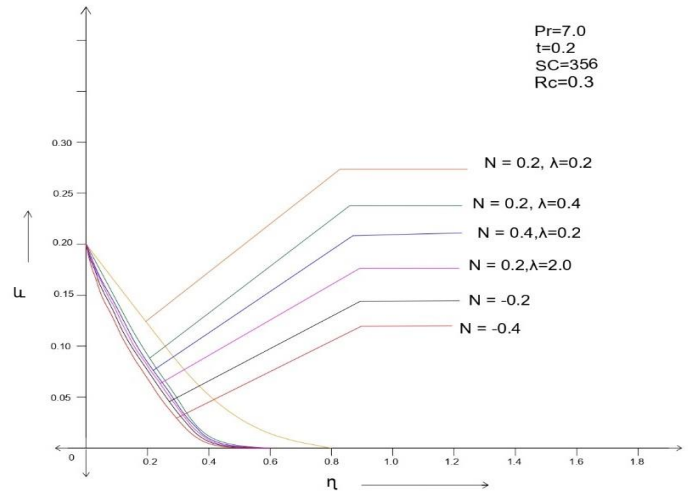

Figure 21 :- As the permeability parameter increases, the axial velocity of water decreases.

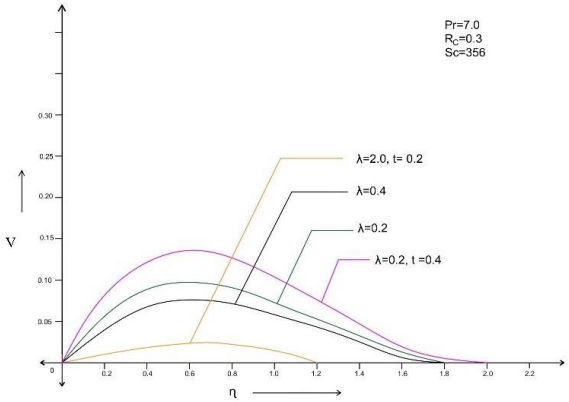

Figure 22 :- As the permeability parameter increases, the magnitude of transverse velocity of water fall down. As time t increases, Transverse velocity increases.

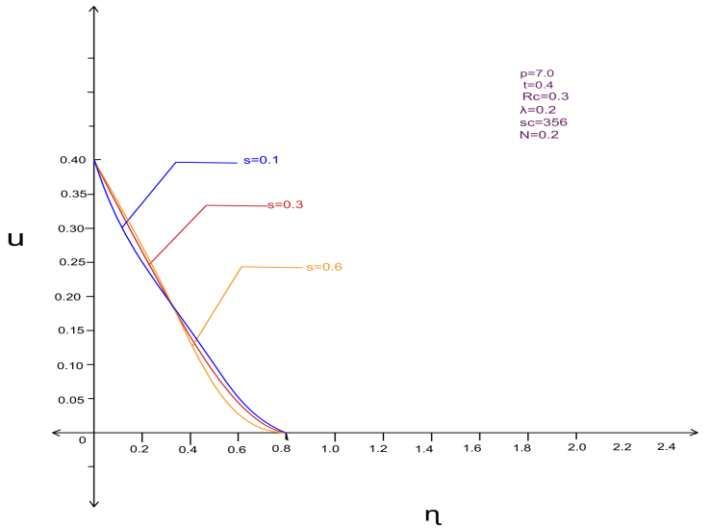

Figure 23:- Heat source S increases flow become unstable for water.

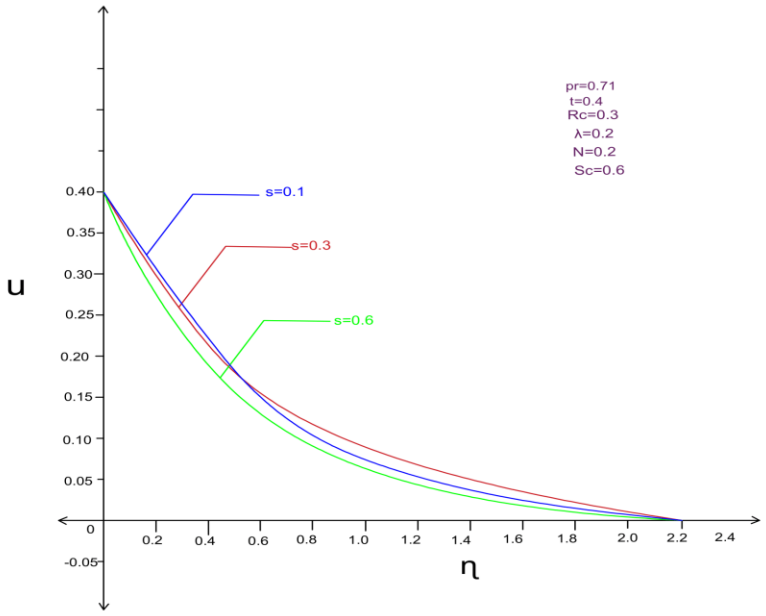

Figure 24:-Axial velocity oscillates as Heat source parameter S increases.

Computed values of τ_x and τ_y (Table 2 and Table 3)

T	Pr	Rc	λ	N	Sc	τ_x	τ_y
0.2	7	0.3	0.2	0.2	152	3.94753367	1.65342678
					356	3.94581708	0.94321784
					453	3.94541269	0.94308983
					617	3.94494494	0.94276531
					750	3.94467738	0.94220503
		0.5			356	4.01337589	0.52719566
		0.7				3.51778293	0.69223905
		0.3	0.4		356	3.71919800	1.07768718
			2.0			3.51957865	1.05473584
			0.2	0.4		4.57468530	1.08735273
				-0.2		2.68808062	0.90674806
				-0.4		2.05921240	0.27321317
0.4	7	0.3	0.2	0.2	356	4.92869209	0.94767043
0.2	7	10^2	0.2	0.2	356	3.97856705	-0.31591443
		10^1				1.64399307	-0.90007510
		10^0				3.27140907	0.44336917
		10^{-1}				5.32347636	1.05346988
		10^{-2}				7.19565042	2.07074822
		10^{-3}				7.20678472	2.26000640

		10^{-4}				7.20396619	2.27454159
		10^{-5}				7.20364416	2.27455491
		10^{-6}				7.20361154	2.27410090
0.2	100	0.3	0.2	0.2	356	3.78913449	0.70511119

T	Pr	Rc	λ	S	N	Sc	τ_x	τ_y
0.2	0.71	0.3	0.2		0.2	0.22	8.72634025	-3.32143931
						0.60	8.43164119	-3.58465353
						0.78	8.21109929	-3.38993153
						0.94	7.45764480	-4.27511385
						0.99	8.22203618	-3.31412186
		0.5				0.6	13.26639627	-2.83727435
		0.7					-3.53832428	10.81065909
		0.3		0.1			0.91612810	-4.36909102
				0.3			13.01820262	-14.98411523
				0.6			14.59565062	-8.73100578
			0.4			0.6	7.70649549	-2.47376135
			2.0				5.14033348	-0.42251125
			0.2		0.4	0.6	7.25574330	-4.10589876
					-0.2		9.78343695	-1.94216307
					-0.4		9.95933483	-1.22091785
0.4			0.2		0.2	0.6	9.78482218	-3.81816558
0.2	0.71	10^2	0.2		0.2	0.6	22.22201477	-8.32261941
		10^1					1.81142640	-5.82606333
		10^0					1.93021216	2.79472764
		10^{-1}					9.37603321	-1.80237785
		10^{-2}					11.45695236	-0.28481582
		10^{-3}					11.49944161	-0.02868229
		10^{-4}					11.49987082	-0.00285806
		10^{-5}					11.49987511	-0.00027543
		10^{-6}					11.49987516	-0.00001716
0.2	0.1	0.3	0.2		0.2	0.6	15.29760983	0.93449258

4. Conclusion

When all other parameters are held constant, axial velocities are displayed for a range of Schmidt number values. The axial velocities of air and water are found to decrease as Sc increases. As time t increases, the axial velocity increases, and the magnitude of the air's transverse velocity increases with increasing time t. When Rc decreases for air and water, flow become unstable. For air and water, as heat source S increases, axial velocity oscillates (flow become irregular)

For air, both axial and transverse skin friction become unstable as the rotation parameter Rc rises. However, transverse skin friction is irregular for water and axial skin friction increases as Rc increases. Axial and transverse skin friction decrease with increasing permeability parameter λ for water, but they increase with decreasing permeability parameter λ for air. As the Prandtl number Pr increases, the axial velocity falls. The table also shows that, except for methanol, a rise in Sc causes the transverse velocity of air to become unstable, whereas an increase in Sc causes the axial friction and transverse skin friction of water both decreases. As heat source S grows, axial skin friction rises, but transverse skin friction becomes unstable.

References:

[1] Stokes, G.C.: On the effect of the internal friction of fluids on the motion of pendulum. Camb. Phil.Trans., IX, (1851) 8

[2] Stewartson, K.: On the impulsive motion of a flat plate in a viscous fluid. Quart. J. Appl. Math 4 (1951) 182.

[3] Stewartson, K.: On the impulsive motion of a flat plate in a viscous fluid. Quart. J. Appl. Math 22 (1973) 143

[4] Hall, M.G.: Boundary layer over an impulsively started flat plate. Proc. Roy. Soc. Landon, 310 A (1969) 401.

[5] Tani, I and J.J. Yu: Unsteady boundary layer over a flat plate started from rest. Recent Research on unsteady boundary layers. IUTAM Symp., 1971, vol 1 (1971) 886.

[6] Gebhart, B., Heat Transfer ,2nd ed.., New York: McGraw-Hill,1971

[7] Bejan a. Convective Heat Transfer in porous Media, New York: John Wiley and Sons,198

[8] Soundalgekar, V.M., Free convection effects on the Stokes problem for an infinite vertical plate J. Heat Transfer (Tr.ASME)99C (1977)499.

[9] Park C.W. and Lau S.C., Effect of Channel Orientation of Local Heat (Mass) Transfer Distributions in a Rotating Two-Pass Square Channel with Smooth Walls, J. Heat Tansf. Vol 120, no. 3, pp. 624-632,1998.

[10] Bhalerao V.B. and Lahurikar R.M. Mass Transfer Effects on Transient Free Convection Flow past an Infinite Vertical Plate in Rotating Fluid, Int.j. Math. Sci. Eng. Appl., vol. 8, no.2, pp. 367-372,2014.

[11] Vadasz, P., Coriolis Effects on Gravity Driven Convection in Rotating Porous Layer Heated from 11, Below, J. Fluid Mech., vol.376.pp 351-375,1998

[12] Bejan, A., Convection Heat Transfer, 4th ed. New York: John Wiley and Sons,2013.

[13] Srinivasa Raju, R., Sudhakar, K., and Rangamma, M., The Effect of Thermal Radiation and Heat Source on an Unsteady MHD Free Convection Flow past an Infinite Vertical Plate with Thermal Diffusion and Diffusion Thermo, J. Inst. Eng. IndiaSer. C, vol 94, pp.175-186,2013

[14] Srinivasa Raju R. and Gorla R.S.R., Analytical and Numerical study of Unsteady MHD Free Convection Flow over an Exponentially Moving Vertical Plate with Heat Absorption, Int. J. Therm. Sci., vol. 107, pp. 303-315,2016

[15] Sheri S.R. and Srinivasa Raju, R., Transient MHD Free Convection Flow past an Infinite Vertical Plate Embedded in a Porous Medium with viscous Dissipation, Meccania, vol.5.1, no.5, pp.-1057-1068,2016.

[16] Srinivasa Raju, R., Mahesh Reddy, B., Rashidi, M.M., and Gorla, R.S.R., Application of Finite Element Method to Unsteady MHD Free Convection Flow past a Vertically Inclined Porous Plate including Thermal Diffusion and Diffusion Thermo Effects, J. Porous Media, Vol.19, no. 8, pp701-722,2016 c.

[17] Srinivasa Raju. R, Jitender Reddy Reddy, G, Anand Rao, J., and Rashidi M. M., Thermal Diffusion and Diffusion Thermo Effects on an Unsteady Heat and Mass Transfer MHD Natural Convection Couette Flow using FEM, J. Comput. Des. Eng., vol. 3, no.4. pp. 349-362 ,2016a

[18] Reddy J.G., Srinivasa Raju, R., Manideep P., Rao j., Thermal Diffusion and Diffusion Thermo Effects on Unsteady MHD Fluid Flow past a Moving Plate Embedded in Porous Medium in the Presence of Hall Current and Rotating System, Trans. A. Razmadze Math. Inst. J., VOL. 170, pp. 243-265,2016.

[19] Srinivasa Raju. R., Aruna, G., Swamy Naidu, N., Varma, S.V.L., and Rashidi M.M., Chemically Reacting Fluid Flow Induced by an Exponentially Accelerated Infinite Vertical Plate in a Magnetic Field and Variable temperature via LTT FEM, Theor. Appl. Mech., vol. 43, no. 1, pp.49-83, 2016b.

[20] Dodda R., Srinivasa Raju R and Anand Rao J., Influence of Chemical Reaction on MHD Boundary Layer Flow of Nanofluid over a Nonlinear Stretching Sheet with Thermal Radiation, J. Nanofluids, vol.5, no.6, pp. 880-888, 2016.

[21] Soundalgekar, V.M. and S.K. Gupta: Effects of free convection currents on the flow past an accelerated vertical plate. Acta Cien. Indica 6 (1980)138.

[22] Gebhart B., Y. Jaluria, R.L. Mahajan and B. Sammakia: Buoyancy-induced flows and transport. Reference Edition. Heidelberg: Springer-Verlag 1988.

[23] Gebhart B. and L. Pera: The nature of vertical natural convection flows resulting from the combined buoyancy effects of thermal and mass diffusion. International J. Heat Mass Transfer 14 (1971) 2025.

[24] Lahurikar R. M., Gitte V. T., Ubale Patil P.P. (2018) "Mass transfer effects on flow through porous medium past an impulsively started infinite vertical plate in a rotating fluid". Int. J. of Fluid Mechanics Research ,45(4):321-338(2018)

[25] Soundalgekar V.M., Pohanerkar S. G .and Lahurikar R. M. (1992) "Effect of mass transfer and heat sources on the flow past an accelerated infinite vertical plate" forschung im ingenieurwesen-Engineering Research Bd. 58 Nr 3, p.63-66.

[26] Lahurikar R.M., Gitte V.T., Ubale Patil P.P. (2017) "Mass Transfer Effects on Stokes Problem for an Infinite Vertical Plate in a Rotating Fluid" Int. J. of Engg. Research and Application.Vol.7, Issue 7(part 2) July 2017.pp 01-09

[27] Muskat, M., Flow of Homogenous Fluids through Porous Medium, Ann Arbor, MI: J.W. Edwards Inc., 1946

[28] Lahurikar, R.M. Formulae for complex Error Function. Bulletin Marathwada Math. Soc., vol. 15, no.2, pp. 42-48, 2014.